Int J Adv Manuf Technol (2016) 85:1315–1323
DOI 10.1007/s00170-015-8022-1

ORIGINAL ARTICLE

Machinability of plunge milling for damage-tolerant titanium alloy TC21

Tao Sun[1,2] · Yu-can Fu[1] · Lei He[1] · Xue-mei Chen[3] · Wen-guang Zhang[3] · Wei Chen[3] · Xu-bin Su[3]

Received: 11 June 2015 / Accepted: 25 October 2015 / Published online: 5 November 2015

Abstract Damage-tolerant titanium alloy, TC21, is widely used for the important components of the new-generation aircraft with high strength and durability requirements, many of which are machined by plunge milling. For optimizing the plunge milling parameters and improving machining efficiency, a number of experiments were carried out to study the machinability of plunge milling TC21. The effects of plunge milling parameters on cutting forces, the cutting temperature, and the tool life were investigated and analyzed. The process of the tool failure and the mechanism of tool wear were explored. Results showed that the cutting temperature had more influence than cutting force under the same parameters, and higher cutting heat was the main reason of the tool failure. In addition, this study showed that a large fracture of insert corner was the form of final tool failure. Furthermore, the results indicated that TiAlN-coating tool was more suitable for plunge milling TC21 than TiN-coating tool, and abrasive wear and adhesive wear were the main reasons of tool wear. Finally, reasonable parameters of plunge milling TC21 were recommended. Thus, a cutting tool with proper plunge milling parameters and tool materials should be carefully chosen to satisfy the tool life in real production.

✉ Yu-can Fu
yucanfu@nuaa.edu.cn

[1] College of Mechanical and Electrical Engineering, Nanjing University of Aeronautics and Astronautics, Nanjing 210016, China

[2] School of Mechanical and Electrical Engineering, Xuzhou Institute of Technology, Xuzhou 221111, China

[3] Chengdu Aircraft Industry (group) Co., Ltd., Chengdu 610000, China

Keywords Damage-tolerant titanium alloy · Plunge milling · Machinability · Tool life · Mechanism of tool wear

1 Introduction

As an α+β titanium alloy with the nominal composition of Ti–Al–Sn–Zr–Mo–Cr–Si–Nb, damage-tolerant titanium TC21 has excellent integrated mechanical properties, such as high-fracture toughness, high strength, excellent crack resistance ability, and thermal-stability [1–3]. Therefore, TC21 is widely used for manufacturing important components of the new-generation aircraft.

Machinability of TC21 is an important issue which needs more considerations for the widespread use of TC21. So far, there has been limited literature for machinability of TC21, and most efforts were concentrated on side milling. Shi et al. [4, 5] investigated the machinability of TC21 and found that tool life in side-milling TC21 is much shorter than that in milling TC4. In order to improve the machinability of TC21, Yu et al. [6] changed the hydrogen content of TC21. It was found that cutting forces and surface roughness was reduced, and chip breaking became easier with the hydrogen content in the range of 0.25–0.3 %. Zhou and Li [7] proposed that smaller amount of cutting depth, larger cutting speed, and radial cutting width should be used during side-milling TC21 based on orthogonal test and range analyses of surface roughness. By using ((Ti, Al)N-TiN)-coated carbide tools in high-speed side-milling TC21, Zhang et al. [8] investigated the effects of cutting forces and wear mechanism under different cutting conditions. Their researches showed that adhesion wear mainly caused chipping along the flank and rake faces, which was identified as the main factor of coated carbide tool failure.

Recently, plunge milling operation has gained great attention as a promising roughing process. Since the feed axis

coincides with the most rigid spindle axis direction, the process tends to be more vibration-free than side-milling operations. As a result, plunge milling could reduce the deformation of a workpiece and improve the machining efficiency. For the reason, plunge milling recently became popular in roughing of cavities in the die, mold, and aerospace industries [9, 10].

There have been significant researches for the mechanics and dynamics of plunge milling operations. To improve the stability of plunge milling, Hoon-Ko and Altintas [9, 10] applied time domain modeling of the mechanics and dynamics of the plunge milling process considering the rigid body motion of the cutter and three translational and torsional vibrations of the structure. In another study by Hoon-Ko [11], the aforementioned model was used considering cutting edge radius and dynamic motion of cutter center. Damir et al. [12] studied the dynamics of the plunge milling process for systems with a rigid and flexible work piece using the time domain simulation model. Their model predicted the cutting forces, system vibration as a function of work piece and tool dynamics, tool setting errors, and tool kinematics and geometry. Rauch and Hascoct [13] proposed a new approach to enhance the implementation of plunge milling tool paths by computing the achievable material removal rate according to the tool path parameterization, the machine tool dynamics, and the machined feature properties. Zhuang et al. [14] demonstrated a new cutting model to predict the plunge milling force based on the precise plunge milling geometry. In this model, the cutting step and radial cutting width were taken into account for chip thickness calculation.

Nowadays, TC21 has been employed to manufacture many components of aviation aircraft, such as the joints of the wing and aero-engine pylon and connecting frames of the fuselage and undercarriage, etc. The aforementioned components are widely produced by using plunge milling. Therefore, it is very important to perform research on plunge milling of TC21. In practical plunge milling process, the machinability is an overarching concern for all engineers. As a result, study on the machinability of plunge milling of TC21 is important. In this paper, the effects of plunge milling parameters on cutting force, cutting temperature, and tool life are investigated. In addition, the process of tool failure and the mechanisms of tool wear are discussed. The aims of this paper are to provide theoretical and experimental basis for improving the cutting efficiency and tool life of plunge milling TC21.

2 Experiment setup and procedures

Work piece material The experiment material was a 100-mm diameter bar. The initial microstructure after quasi-β forging and double annealing processing consisted of basket-weave structure, as shown in Fig. 1.

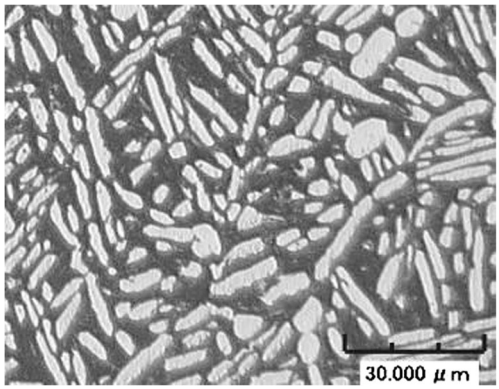

Fig. 1 Microstructure of raw material TC21

The chemical composition and major performance of TC21 are given in Tables 1 and 2, respectively.

Machine tool and measurement method The experiment was carried out using Mikron UCP 710, which is a five-axis machining center with maximum rotational speed of 18,000 rpm, feed rate up to 20 m/min, and rated power of 15 kW.

Cutting forces were measured by a Kistler 9265B three-piezoelectric dynamometer, the matching Kistler 5019A charge amplifier, and the corresponding data acquisition and processing system. Semi-artificial thermocouple technique was used to measure the cutting edge temperature. A suitable insulated constantan wire was implanted into the work piece. When the work piece with the constantan wire was cut, an instantaneous hot junction is formed and the generated electromotive force can be detected. Then, the cutting temperature was calculated according to the calibration data which was obtained before. Figure 2 shows the experimental method of plunge milling.

Flank wear was measured by a KH-7700 digital microscope system and an INSPEC scanning electron microscope (SEM) equipped with an OXFORD X-act/INCA150 energy-dispersive X-ray spectroscopy (EDX).

Cutting tools A cutting tool used in all experiments was provided by Sandvik, which includes an insert and a toolholder, as shown in Fig. 3. The main specifications of the insert are as follows: ISO standard is R210-09 04 12M-MM 2030, the rake angle was 0°, the clearance angle was 7°. As a double-coated cutting tool has been used, the coating material was consisted of TiN and TiAlN as outer and inner coatings, respectively. It is worth mentioning that only one insert was used. The main specifications of the toolholder are as follows: ISO standard is

Table 1 The chemical compositions of TC21 (in weight percent) [15]

Si	Cr	Zr	Nb	Sn	Mo	Al	Ti
0.09	0.77	2.19	2.31	2.32	2.87	6.78	Balance

Table 2 The main physical properties of TC21 [15]

Tensile strength σ_b (MPa)	Yield strength $\sigma_{0.2}$ (MPa)	Elongation δ_5 (%)	Percentage of area reduction ψ (%)	Plane strain fracture toughness $K_{IC}(MPa\cdot\sqrt{m})$
1174	1083	11.3	20	90.6

R210-03 2A25-09M, the maximum cutting diameter is 32 mm, and the connection diameter is 25 mm.

The corner and bottom parts of the tool insert are used for cutting in plunge milling. Thus, the wear of the flank face of the bottom cutting edge is considered as the failure standard of the tool. For instance, average flank wear will be above 0.4 mm if the wear of the bottom cutting edge's flank face is evenly distributed. On the other hand, maximum flank wear should be above 0.6 mm if the wear is not evenly distributed. The length of tipping becomes over 0.6 mm if the insert has tipping.

Cutting parameters The plunge milling contains four parameters: cutting speed v_c, feed per tooth f, radial cutting depth a_e, and step interval s. Table 3 indicates the cutting parameters used in the plunge milling experiments.

3 Results and discussions

Cutting force Figure 4 shows the original signals of plunge milling force. The signals illustrate that the volatility of cutting force is so large that the corresponding mechanical impact should be fairly high.

Figures 5, 6, and 7 show the effects of the plunge milling parameters, such as v_c, f, and a_e on three cutting forces. It is evident that the axial force F_z is maximum, the tangential force F_x is minimum, and the radial force F_y is greater than F_x but less than F_z. While the resultant force F_r is slowly decreasing with the rise of v_c, the resultant force responds oppositely with the rise of f. Besides, it is obvious that a_e has a more pronounced effect on cutting force than v_c and f.

The following reasons can be used to explain the effect of cutting speed on cutting force for plunge milling TC21. On one hand, with increasing cutting speed v_c, the degree of strain-hardening and deformation resistance of shearing field is increasing that increases the cutting force. On the other hand, a higher temperature is produced with increasing v_c. The softening effect on working material will also be increased with increasing temperature. This causes the decrease of material's friction coefficient, strength, and hardness; thus, cutting force decreases. Since the effect of softening is stronger than the degree of strain-hardening, the cutting force is slowly reduced with the increase of v_c.

There are a couple of reasons behind the variation of cutting force in feed per tooth for plunge milling TC21. Firstly, cutting power and cutting force are increasing with increasing feed per tooth f. Secondly, the area of residual metal also increases with the increase of f. However, this will increase the extrusion pressure for tool. The orientation of extrusion pressure is opposite the orientation of cutting force and offset

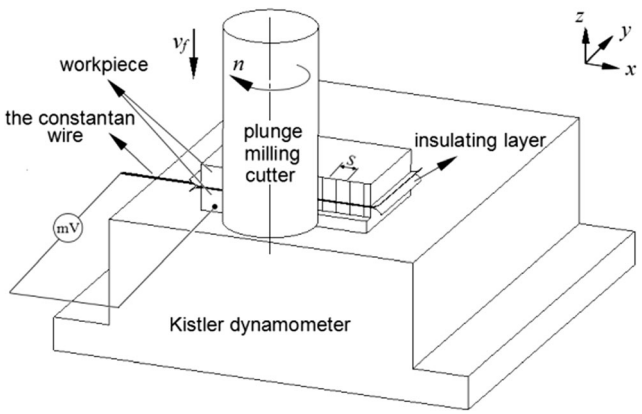

Fig. 2 Schematic diagram of the plunge milling

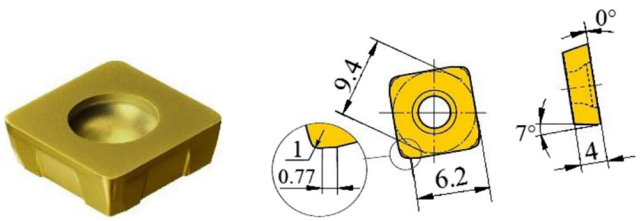

(a) R210-09 04 12M-MM 2030 insert

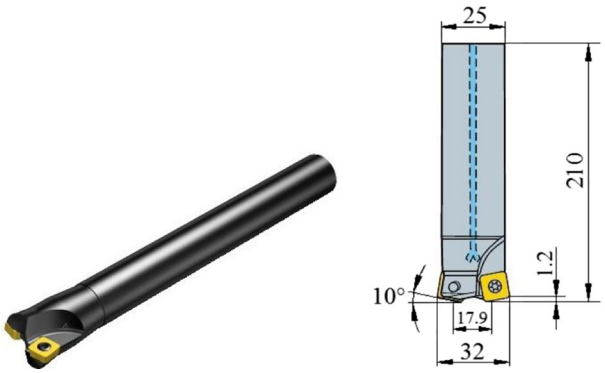

(b) R210-03 2A25-09M toolholder

Fig. 3 Information of the insert and toolholder

Table 3 Cutting parameters used in plunge milling experiments

v_c (m/min)	f (mm/tooth)	a_e (mm)	s (mm)
30	0.08	2	5
40	0.1	4	
50	0.12	6	
60			

the part of cutting force. Consequently, there is no significant change observed in the cutting forces with the increase of f.

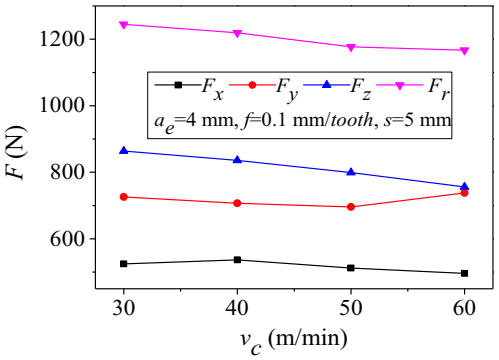

Fig. 5 Effect of cutting speed on cutting force

Cutting temperature The influence of cutting parameters, such as v_c, f, and a_e on cutting edge temperature, was investigated.

Figure 8 shows the measured original electromotive force signal of plunge milling temperature by semi-artificial thermocouple technique. Through the technique of thermocouple calibration, the relation of electromotive force and temperature for a TC21-constantan thermocouple can be obtained, as shown in Fig. 9. Then, the cutting temperature can be calculated by contrasting the maximum peak of original electromotive force signal with relation of electromotive force and temperature. For example, Fig. 8 shows that maximum peak of the original signal is 22 mV, by contrasting the relation of electromotive force and temperature as shown in Fig. 9; finally, cutting temperature is calculated as 545 °C in the condition of v_c=40 m/min, f=0.1 mm/tooth, and a_e=4 mm.

Figures 10, 11, and 12 show the effect of v_c, f, and a_e on cutting edge temperature. The upward trend of cutting temperature with increasing the v_c, f, and a_e is very obvious. It is worth mentioning that the temperature rises abruptly with increasing v_c from 30 to 40 m/min and then it goes slowly up, as shown in Fig. 10. In addition, the maximum and minimum temperature was recorded to be 682 and 376 °C.

It is believed that cutting power increases with increasing cutting speed v_c. More cutting energy with increasing cutting power will be transformed into heat. Meanwhile, faster flow speed of chip will lead to increase frictional heat between tool and chip. As a result, cutting temperature rises obviously with increasing v_c.

There are two obvious reasons for increasing the cutting temperature with respect to feed per tooth f. Firstly, increased cutting energy with increasing f will generate more cutting temperature. Secondly, increased residual metal area with increasing f will significantly increase the extrusion and friction, which ultimately will increase cutting temperature.

Tool life Figure 13 reveals the tool life using a different v_c under the fixed condition: a_e=4 mm and f=0.1 mm/tooth. It can be commented that the cutting speed has great influence on tool life. Using v_c=30 and 50 m/min, the cutting length was reached to be 3.1 and 0.5 m, respectively.

Figure 14 shows the effect of f on tool life. In the case of v_c=40 m/min and a_e=4 mm, the cutting length was found to be 1.3 and 0.7 m using f=0.08 and 0.12 mm/tooth that indicates effect of feed per tooth on tool life is not significant.

Figure 15 demonstrates the effect of a_e on tool life. It is evident that radial cutting depth has significant influence on tool life. For example, cutting length was found to be 2.2 and 0.2 using the radial cutting depth of a_e=2 and 6 mm, respectively.

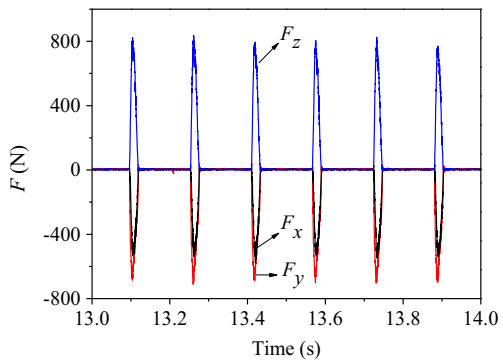

Fig. 4 Original signal of the plunge milling force (v_c=40 m/min, f=0.1 mm/tooth, and a_e=4 mm)

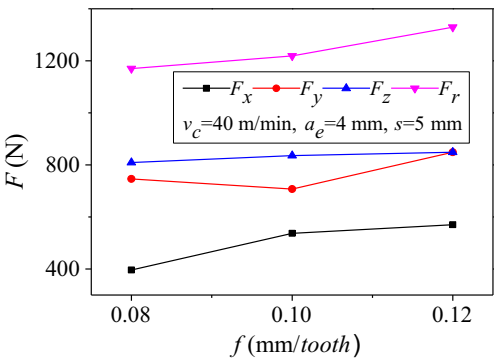

Fig. 6 Effect of feed per tooth on cutting force

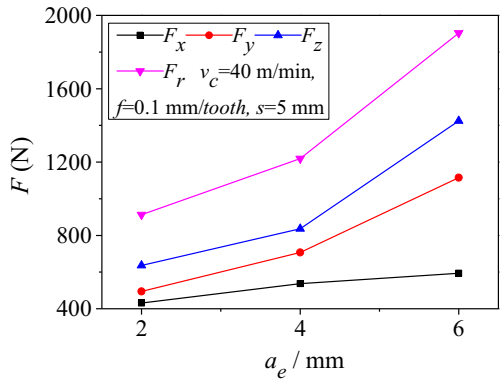

Fig. 7 Effect of radial cutting depth on cutting force

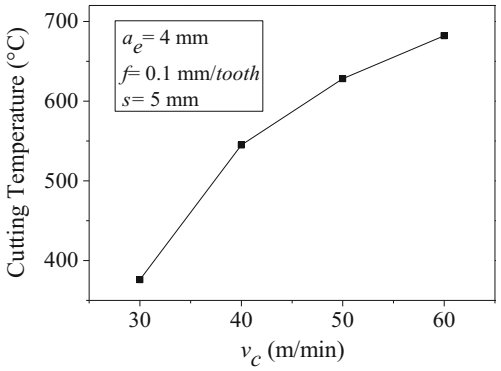

Fig. 10 Effect of cutting speed on cutting edge temperature

As shown in Figs. 7 and 12, using v_c=40 m/min, f= 0.1 mm/tooth, and a_e=2 mm, the resultant cutting force and temperature were obtained to be 913 N and 420 °C, respectively. On the other way, changing the parameters to v_c=30 m/min and a_e=4 mm, the resultant cutting force and temperature were achieved 1245 N and temperature 376 °C, respectively, as shown in Figs. 5 and 10. Consequently, tool life in terms of cutting length was measured to be 2.2 and 3.1 m for the first and second set of parameters, respectively. These illustrate that cutting heat plays a major role in tool failure.

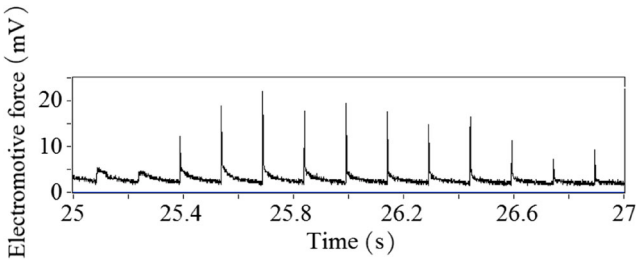

Fig. 8 Original signal of electromotive force (v_c=40 m/min, f=0.1 mm/tooth, and a_e=4 mm)

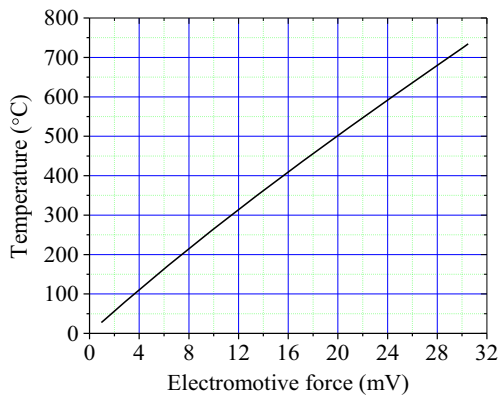

Fig. 9 Relation of electromotive force and temperature for TC21-constantan

The aforementioned tool life figures indicate that the tool life of plunge milling TC21 are not too long under the particular cutting parameters. Plunge milling is not only an interrupt cutting process but also rough machining. Thus, mechanical impact and thermal impact are considerably high with high cutting force and temperature, which affects the tool life.

Therefore, based on the aforementioned discussions, the following plunge milling parameters are recommended for TC21 alloy: (i) cutting speed, v_c=30–40 m/min; (ii) feed rate, f=0.08 to 0.12 mm/tooth, and (iii) radial cutting depth, a_e= one sixteenth to one eighth of tool diameter.

Process of tool failure From Figs. 13, 14, 15, it can be seen that all the curves basically overlap at a particular condition, such as the curves of initial wear stages (0.2 mm) using three v_c under a_e=4 mm and f=0.1 mm/tooth (Fig. 13). This situation is related to coating materials of insert. The insert is made of double coatings, the where outer coating consists of TiN and the inner one is TiAlN. It is worth mentioning that TiAlN coating has better physical and mechanical performances than TiN-coating, as shown in Table 4.

During the plunge milling for TC21, the cutting temperatures (376 to 682 °C) were high enough to exceed the tolerable temperature of the TiN-coating (500 °C), which will lead to

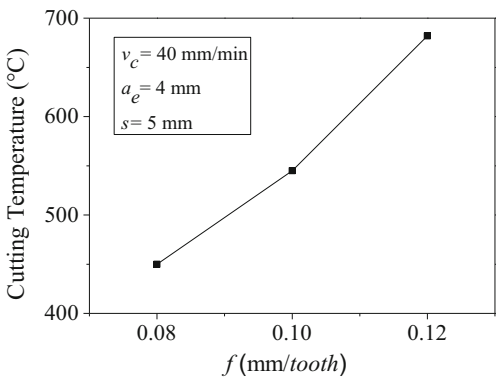

Fig. 11 Effect of feed per tooth on cutting edge temperature

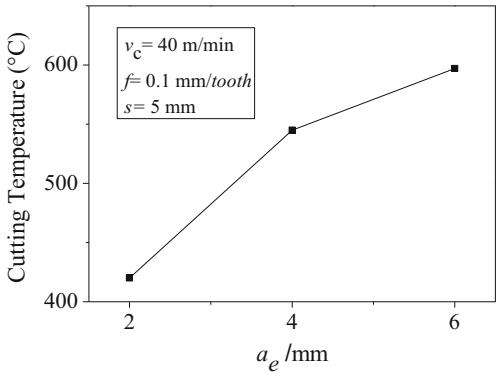

Fig. 12 Effect of radial cutting depth on cutting edge temperature

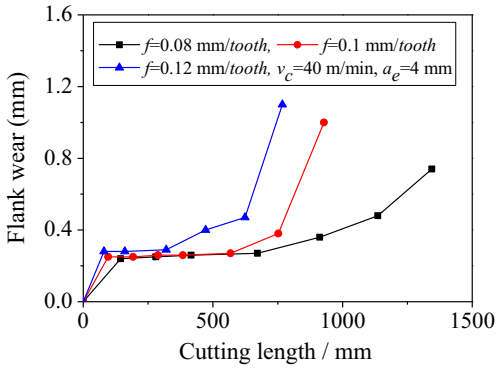

Fig. 14 Effect of feed per tooth on tool life

ablation of the outer TiN coating. This causes the physical performance of the outer coating weakening and the wear speeding up. It can be found that the ablation regions always exist from initial wear stage until failure during plunge milling of TC21, as shown in Fig. 16. During initial stage of wear, the outer coating is quickly worn because of ablation as shown in Fig. 16a, b, and so tool wear curves basically overlap at a particular condition.

Subsequently, being into normal wear stage, the inner TiAlN coating is used for cutting. The flank wear appears so slow that the cutting length is extended due to the excellent physical performance of TiAlN coating. As shown in Fig. 16c, when the cutting length appeared to be 2.4 m, the corner displayed a fragmentation. As a result, the wear of tool flank increases to 0.4 mm.

During rapid wear stage, the cutting force and heat increase rapidly because wear and fragmentation of tool increase. High cutting heat will accelerate softening of the tool material. Furthermore, fatigue fracture of tool is also affected through increasing mechanical and thermal impact. Finally, the fragmentation of insert corner is turned into a large fracture within a short time. As shown in Fig. 16d, when the cutting length becomes 3.1 m, the insert corner shows a large fracture resulting in tool failure.

Mechanism of tool wear To investigate the mechanism of tool wear in plunge milling TC21, the earlier and later stages of tool wear were observed using SEM under the condition of v=40 m/min, a_e=4 mm, f=0.12 mm/tooth and s=5 mm.

At the earlier stage of tool wear, the coating material still exists. As shown in Fig. 17, the abrasive wear is not obvious because the hardness of coating materials is much higher than hard spots of workpiece and fragments of built-up edge.

At the later stage of tool wear, the coating material basically vanishes and temperature increases rapidly in response of large wear. The higher temperature leads to the reduction of hardness of tool material, which will aggravate the scratch on the tool flank. Hence, striations perpendicular to cutting edge is clearly visible in Fig. 18. This illustrates that the abrasive wear obviously occurs in flank of insert.

In order to confirm the adhesive wear in the earlier stage of tool wear, energy-dispersive X-ray spectroscopy (EDX) was taken from two points in Fig. 17. The chemical composition of the points is shown in Table 5. The EDX results show that two points are adhesive regions of titanium because their composition contains large amounts of titanium. Thus, the adhesive wear exists on flank of insert in the earlier stage of tool wear.

At a later stage of tool wear, increasing wear aggravates the mechanical impact of the insert corner which makes the adhesive material quickly peel off (Fig. 18). Hence, adhesive

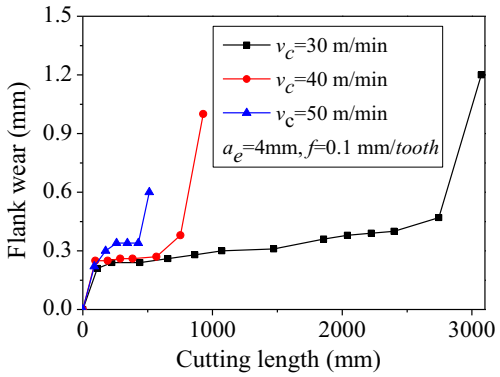

Fig. 13 Effect of cutting speed on tool life

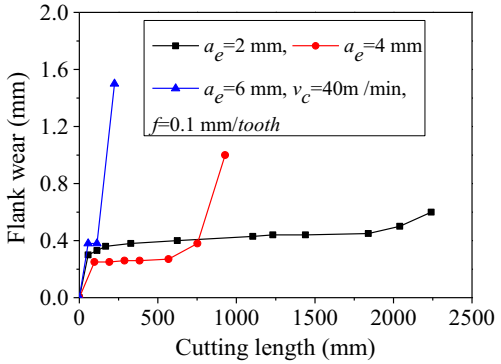

Fig. 15 Effect of radial cutting depth on tool life

Table 4 The main physical properties of TiN and TiAlN coating [16]

Coating material	Tolerable temperature (°C)	Elasticity modulus (GPa)	Hardness (HV)
TiN	500	260	2300
TiAlN	800	400	3300

materials are not obviously discovered on the flank of insert corner. However, on the flank away from the corner of insert, it is evident that pronounced adhesive materials are visible (Fig. 19), which could be also confirmed in EDX results (Table 6 and Fig. 20).

Adhesion of titanium alloy is mainly due to its lower hardness, higher chemical reactivity, and stronger affinity than tool material under high temperature and pressure conditions. When adhesion occurs to a certain degree, stripping of adhesive layer will happen to form the adhesion wear. This will be responsible for cutting tool failure process.

The presence of oxygen element in Tables 5 and 6 indicates that oxidation occurred on the flank of insert. During plunge milling process, a large mechanical impact leads to rapid stripping of outer TiN coating at a higher cutting edge temperature.

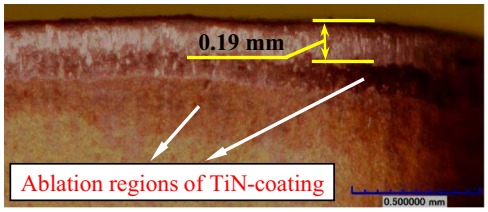

(a) Cutting length=0.1 m and VB=0.19 mm (100×)

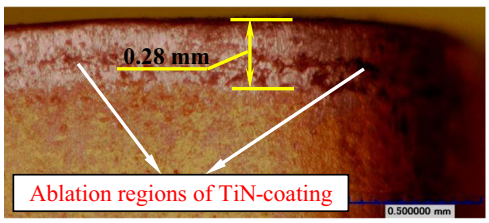

(b) Cutting length=0.9 m and VB=0.28 mm (100×)

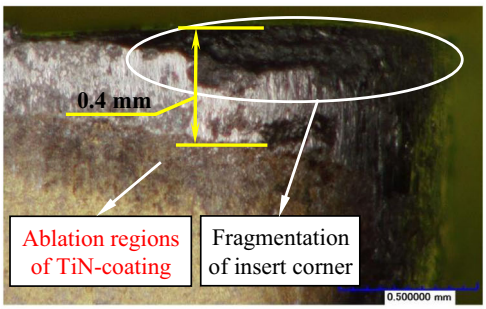

(c) Cutting length=2.4 m and VB=0.4 mm (100×)

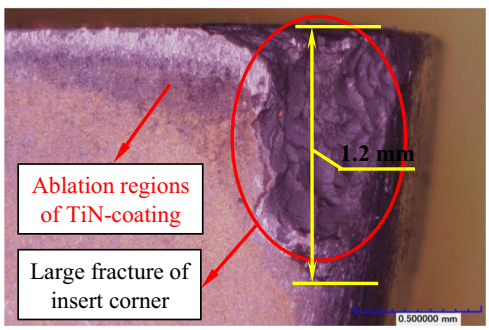

(d) Cutting length=3.1 m and the tool is failure (100×)

Fig. 16 Failure process of the insert for plunge milling (v_c=30 m/min, a_e=4 mm, and f=0.1 mm/tooth)

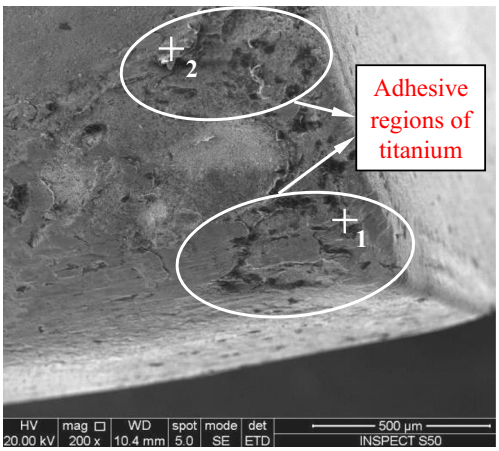

Fig. 17 SEM image of the flank in the earlier stage of tool wear

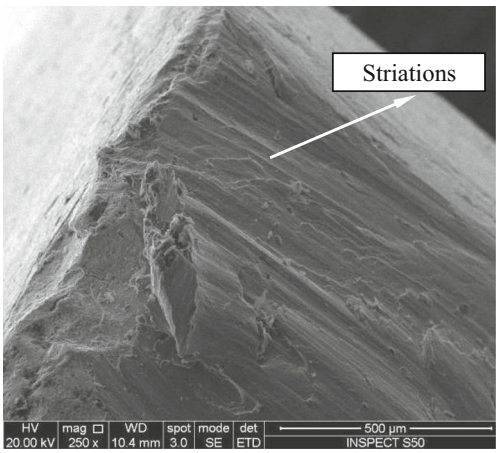

Fig. 18 SEM image of the insert corner in the later stage of tool wear

Table 5 Chemical composition of two points (in weight percent)

Element distribution of the first point							
Cl	Co	Cr	Sn	W	Al	C	Ti
0.45	0.66	1.6	1.98	3.28	4.77	9.18	78.08
Element distribution of the second point							
Al	Na	K	Cl	Ca	W	O	C	Ti
0.59	0.66	0.73	1.02	1.51	6.02	23.1	25.68	40.69

When the inner TiAlN coating cut TC21 alloy, aluminum atoms of TiAlN coating spread outward and unite with atmospheric oxygen atom to form dense Al_2O_3 protective shield. The shield will prevent oxygen element from spreading inward into coating, which improve antioxidant properties for TiAlN coating. Again, this shows that TiAlN coating is superior over TiN coating in cutting titanium material.

Plunge milling is an interrupted cutting technology results in higher cutting edge temperature where temperature gradient is very high. Diffusive wear occurs under the combined effect of strong bonding in titanium alloys and high temperature gradient. At this point, titanium of workpiece material will spread to coating and form TiC layer by reacting with carbon atoms of tool material.

According to Tables 5 and 6, it is clear that tool material contains some carbon elements; thus, the occurrence of diffusive wear should be considered. With the action of mechanical force and impact, TiC layer adhesion to tool surface begins to strip and then proceed with a fresh diffusive wear.

Finally, it can be deduced from the aforementioned analyses that both abrasive and adhesive wear play vital roles as the wear mechanism of coating tool. Using proper cutting parameters, tool failure mode is fracture after normal wear of tool. To improve tool life, appropriate cooling methods, or parameters ought to be used to reduce cutting temperature. In addition,

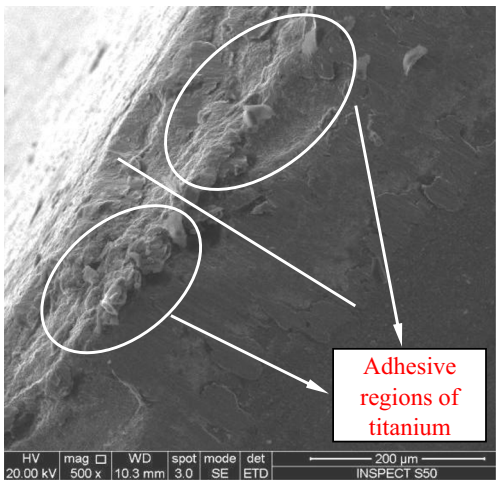

Fig. 19 SEM image of the flank away from insert corner in the later stage of tool wear

Table 6 Chemical composition along the oblique line (in weight percent)

Ca	S	Cr	Co	Al	W	O	C	Ti
0.45	0.55	0.87	1.95	2.59	11.64	12.02	29.33	39.30

more tool inserts or less radial cutting depth can be adopted to decrease mechanical impact.

4 Summary

In this study, machinability of plunge milling for TC21 is discussed. Firstly, for cutting force and cutting temperature, the effects of plunge milling parameters are investigated. Then, the tool life and the process of tool failure are analyzed from point of view of cutting force and temperature. Finally, tool wear mechanism is researched by SEM and EDX means.

From the experimental and analytic results, the following conclusions can be drawn.

1. For cutting force in plunge milling of TC21, the influence of f and v_c on cutting force is insignificant, a_e has more influence than f and v_c. With increasing the cutting parameters, the upward trend of cutting temperature is obvious.
2. Higher cutting heat is the main reason of tool failure. The form of final tool failure is large fracture of insert corner under the action of mechanical and thermal impact.
3. Both abrasive and adhesive wear were the main wear mechanisms of the coating tool in plunge milling TC21 alloy. The abrasive wear will be affected by both the mechanical impact and cutting heat. Adhesive wear existed in the whole cutting process which was severely affected by increasing tool wear. The diffusive wear and oxidation also existed in the process of tool wear. The TiAlN coating assisted to prolong tool life because aluminum atoms of TiAlN coating unite with oxygen atoms to form dense Al_2O_3 protective shield.
4. Using a double-coating tool, the recommended plunge milling parameters of TC21 are as follows: v_c is within the range

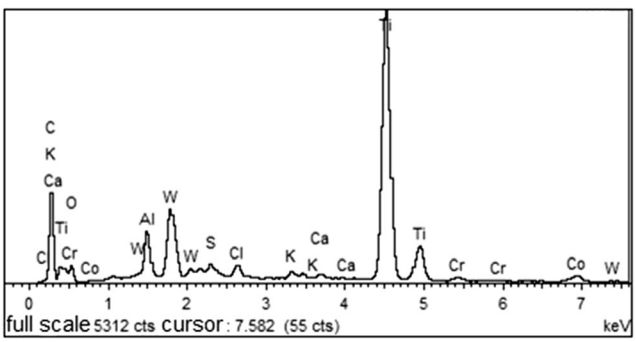

Fig. 20 EDX of selected path in the Fig. 19

of from 30 to 40 m/min, f is from 0.08 to 0.12 mm/tooth, a_e is from one sixteenth to one eighth of tool diameter.

Acknowledgments This work was supported by funding of the Jiangsu Innovation Program for Graduate Education (no. CXLX12_0139). Fundamental Research Funds for the Central Universities is also acknowledged.

References

1. Dang W, Xue XY, Li JS, Hu R, Zhu ZS, Zhang FS, Zhou L (2010) Influence of lamellar microstructure feature on fracture toughness of TC21 alloy. Chin J Nonferrous Metals 20(z1):16–20
2. Yao CS, Chen Z, Wang YX, Zhang J, Du XJ, Chen C (2011) Progress of TC21 titanium alloy in hot working behaviour. Mater Rev 25(23):138–141
3. Zhao JG, Zhang SH, Cheng M, Song HW (2009) Deformation behaviors and microstructure evolution of TC21 alloy in hot working. Chinese Journal of Rare Metals 33(2):153–158
4. Shi Q, He N, Li L, Zhao W, Liu XL (2012) Analysis on surface integrity during high speed milling for new damage-tolerant titanium alloy. Trans Nanjing Univ Aeronaut Astronaut 29(3):222–226
5. Shi Q, Li L, He N, Zhao W, Liu XL (2013) Experimental study in high speed milling of titanium alloy TC21. Int J Adv Manuf Technol 64(1–4):49–54
6. Yu C, Wang Y, Bao YJ, Wang MH (2013) Experimental research on effect of hydrogen on machinability of TC21 alloy. Manuf Technol Mach Tool 10:83–86
7. Zhou C, Li HB (2012) Surface roughness of high-speed milling TC21 titanium alloy. Aerosp Mater Technol 42(6):105–108
8. Zhang HX, Zhao J, Wang FZ, Zhao JB, L AH (2015) Cutting forces and tool failure in high-speed milling of titanium alloy TC21 with coated carbide tools. Proc Inst Mech Eng B J Eng Manuf 229(1): 20–27
9. Jeong HK, Yusuf A (2007) Dynamics and stability of plunge milling operations. Trans ASME 129(1):32–40
10. Jeong HK, Yusuf A (2007) Time domain model of plunge milling operation. Int J Mach Tools Manuf 47(9):1351–1361
11. Jeong HK (2014) Time domain prediction of side and plunge milling stability considering edge radius effect. Procedia CIRP 14(01): 153–158
12. Ahmed D, Eu GN, Mohamed E (2011) Force prediction and stability analysis of plunge milling of systems with rigid and flexible workpiece. Int J Adv Manuf Technol 54(9–12):853–877
13. Matthieu R, Jean YH (2012) Selecting a milling strategy with regard to the machine tool capabilities: application to plunge milling. Int J Adv Manuf Technol 59(1–4):47–54
14. Zhuang KJ, Zhang XM, Zhang D, Ding H (2013) On cutting parameters selection for plunge milling of heat-resistant-super-alloys based on precise cutting geometry. J Mater Process Technol 213(8): 1378–1386
15. Huang X, Zhu ZS, Wang HH (2012). Advanced aeronautical titanium alloys and applications. National Defense Industry Press 2012:157–158
16. Xu YC, Chen KH, Wang SQ, Zhu CJ, Xie CQ, Chen XM (2011) Oxidation and cutting properties of TiN and TiAlN coated cemented carbide. Mater Sci Eng Powder Metall 16(3):425–430